

Stochastic resonance in a nanoscale Y-branch switch

F. Hartmann,^{1,a)} D. Hartmann,¹ P. Kowalzik,¹ A. Forchel,¹ L. Gammaitoni,² and L. Worschech¹

¹Technische Physik, Wilhelm Conrad Röntgen Research Center for Complex Material Systems, Physikalisches Institut, Universität Würzburg, Am Hubland, Bavaria, D-97074 Würzburg, Germany

²Dipartimento di Fisica, NiPS Laboratory, Università di Perugia, I-06123 Perugia, Italy, and Istituto Nazionale di Fisica Nucleare, Sezione di Perugia, I-06123 Perugia, Italy

(Received 18 March 2010; accepted 13 April 2010; published online 30 April 2010)

The self-gating effect in a nanoscale Y-branch switch was exploited to tune the bistable switching so small that noise induced switching occurs. In this regime, the time-dependent response to a weak external periodic signal was studied. The noise-activated switching of the junction was synchronized with the weak external periodic signal due to the presence of the sole internal noise. A maximum synchronization is found and interpreted in terms of stochastic resonance. © 2010 American Institute of Physics. [doi:10.1063/1.3425669]

In commonly used device concepts noise degrades the performance. This is the reason why in designing nanoscale devices significant care is taken in minimizing the effects of intrinsic noise. However, in recent years, a different consideration of the role of noise has arisen that, instead of degrading the device performances, might lead in some cases to enhanced signal to noise ratios. Stochastic resonance (SR) is an example for such a phenomena.¹ SR was first proposed to describe the periodic recurrence of ice ages about every 10⁵ years in terms of a synchronization between the weak modulation of the earth's orbital eccentricity with the earth's climate short-term fluctuations, induced by, e.g., annual solar radiation fluctuations.^{2,3} Since then SR has been applied in a wide variety of systems, e.g., bistable ring laser.⁴ Furthermore, SR was also demonstrated in physiological systems like hair cells⁵ or in neurophysiologic systems like mechanoreceptors in crickets⁶ or crayfishes.⁷ Nowadays SR is commonly invoked when noise and nonlinearity concur to determine an increase in order in the system response.⁸ In this regard the question arises whether or not nanoelectronic systems with a naturally weak response to an external signal compared to the internal noise may show intrinsic nonlinear dynamic characteristics providing noise-enhanced functioning.

Here we present the time-dependent response of a nanoscale Y-branch switch driven in the bistable switching regime caused by the self-gating effect.^{9–11} Proper biasing allows the reduction in the switching hysteresis to be so small, that noise-induced switching occurs. In the regime where the system output is controlled by noise, a weak external periodic signal can be synchronized. An optimum level of synchronization is observed when the time-scale matching condition of SR is achieved.

In Fig. 1(a) an electron microscope image of a Y-branch switch is shown. A modulation-doped GaAs/AlGaAs heterostructure forms the basis of the junction with a two-dimensional electron gas (2-DEG) located 80 nm below the surface. The 2-DEG has a carrier density $n=3.7 \times 10^{11} \text{ cm}^{-2}$ and a mobility $\mu=1.1 \times 10^6 \text{ cm}^2/\text{V s}$ determined by Hall measurements at 4.2 K in the dark. The

Y-branch switch was fabricated with electron-beam lithography and wet chemical etching methods. The left and right side gates are separated by 375 nm wide and 90 nm deep trenches from the central branching junction. For the measurements the barrier-gate voltage V_g was used as input signal and the voltage V_r as output signal as indicated in Fig. 1(a). All measurements were obtained at 20 K in the dark. Supply voltages $V_{lb}=-0.247 \text{ V}$ and $V_{rb}=1.7 \text{ V}$ were applied in series with a load resistor $R_{rb}=10 \text{ M}\Omega$ to the right and $R_{lb}=100 \text{ k}\Omega$ to the left branch, respectively. The stem

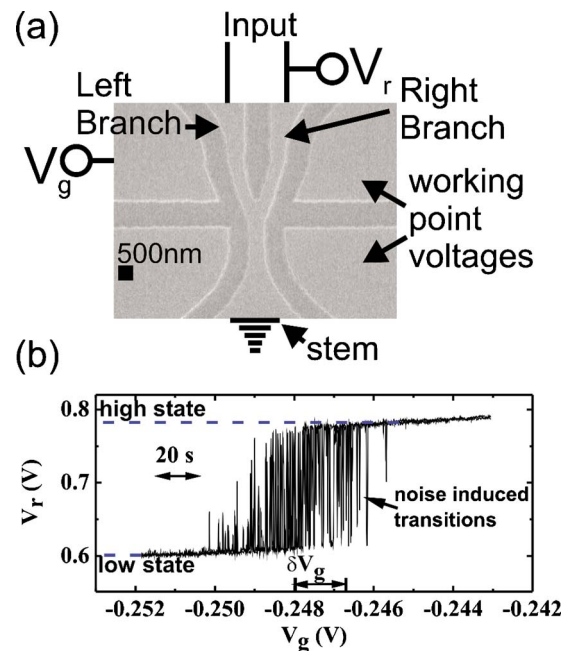


FIG. 1. (Color online) (a) Scanning electron microscopy image of nonlinear mesoscopic three-terminal junction. The voltage drop V_r on the right branch is used as output signal, while the barrier gate voltage V_g is changed. The input voltages $V_{lb}=-0.247 \text{ V}$ and $V_{rb}=1.7 \text{ V}$ as well as the right gate voltage $V_{gr}=2.2 \text{ V}$ set the working condition of the nanojunction. (b) Transfer characteristic of V_r by sweeping V_g . The time between the up and down sweep was set to 20 s. Noise induced transitions from the low L with output $V_r=0.6 \text{ V}$ to the high H with $V_r=0.78 \text{ V}$ state occur within -0.250 and -0.245 V . To measure SR the Y-branch switch is biased at $V_{g,0}=-0.248 \text{ V}$ and additional to the dc component, a weak time periodic signal with amplitude $\delta V_g=1.3 \text{ mV}$ is applied.

^{a)}Electronic mail: fhartmann@physik.uni-wuerzburg.de.

was connected to ground and the right-gate voltage $V_{gr} = 2.2$ V was used to set the working point of the Y-branch switch. In this configuration, the Y-branch switch exhibits bistability due to selfgating.^{9–12} Moreover, as shown in Ref. 13, the internal noise can activate transitions between the two stable states of the bistable Y-branch switch. The resulting transfer characteristic $V_r(V_g)$ is shown in Fig. 1(b). Here V_g was swept forward and backward between $V_g = -0.243$ V and $V_g = -0.252$ V with a sweep rate of $50 \mu\text{V/s}$. Three regions of interest can be identified. At barrier-gate voltages lower than -0.251 V the output of the junction is constant with an output voltage of $V_L = 0.6$ V. This is the stable low state indicated as L. However, for barrier-gate voltages higher than -0.245 V the system changes from V_L to $V_H = 0.78$ V. This is the high state H of the junction. In between these barrier-gate voltages, noise-activated transitions from one stable state to the other occur.

One possibility of recording SR synchronization is based on the mean residence time distribution $N_{H,L}(T)$ of the two stable outputs.¹⁴ The mean residence times of the high H and the low L state $T_{H,L}$ reflect how much time the system spend in each of its respective stable states. For the symmetric case with the gate voltage V_g in the middle of the two threshold values, the system rests equally in each of the two stable states with $T_H = T_L$. Contrary, if the system is not biased symmetrically one of the states is preferred, which results in unequal mean residence times $T_H \neq T_L$. For $V_g = -0.249$ V the low state is the preferred state with $T_L > T_H$, vice versa $T_H > T_L$ for $V_g = -0.247$ V. Usually, to observe SR, a periodic modulation of a subthreshold signal has to be combined with a proper amount of noise. Here we realized a different route. For a given system's noise, the potential was tuned properly to reach SR. For that purpose, V_g was chosen as an input signal with $V_g(t) = V_{g,0} + \delta V_g \sin(\omega t)$, where $V_{g,0}$ is the static dc component. $V_{g,0}$ was set to -0.248 V. For the non-modulated system with $\delta V_g = 0$ V the residence time distribution decays exponentially with time scale T_K ,¹⁵ which is the inverse of the Kramer's rate. T_K can be evaluated by

$$N_{L,H}(T) = \frac{1}{T_K} \exp\left[-\frac{T}{T_K}\right]. \quad (1)$$

In Fig. 2 (top left) $N_L(T)$ is shown without external modulation. The distribution is observed to decay exponentially, as demonstrated by fitted Eq. (1) to the experiment (dashed curve). T_K was determined as $T_K = (0.502 \pm 0.044)$ s. To observe SR, the time-matching condition of SR has to be fulfilled, i.e., $T_\omega = 2T_K$. Indeed, a maximum synchronization for a forcing frequency of $f = 1$ Hz was found.

In contrast to the nonmodulated system, the response of the system to an applied modulation with amplitude $\delta V_g = 1.3$ mV results in a series of peaks at odd multiples of the half value of the periodic time T_ω , i.e., $T = (2n-1)T_\omega/2$ with $n = 1, 2, 3, \dots$. Moreover, it is a characteristic feature of SR that the height of the peaks decreases exponentially with increasing order of n . This is shown in Fig. 2 for $f = 0.1, 0.6, 1.0, 1.8,$ and 2.4 Hz. With modulation the exponential decay distribution passes into a peak distribution, where the height of the peaks decreases exponentially. For $f = 1.0$ Hz, most events are restricted to the first peak at T_K . This observation fits well to the SR time scale condition $T_\omega = 2T_K$. For a shorter modulation time, the system is not always able to

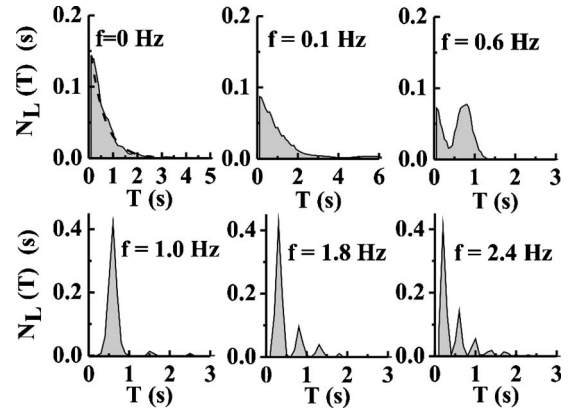


FIG. 2. Normalized mean residence time distribution $N_L(T)$ for the L state for signal frequencies $f = 0, 0.1, 0.6, 1, 1.8,$ and 2.4 Hz. For the nonmodulated system with $f = 0$ Hz the residence time distribution is exponentially decreasing. With Eq. (1) T_K the inverse of the Kramer's rate can be calculated. Below the optimum synchronization frequency of $f = 1$ Hz the distribution is mainly noise controlled. By contrast, at higher frequencies $f = 1.8$ and 2.4 Hz the distributions show higher order peaks at $T = (2n-1)T_\omega/2$, which peaks decrease with higher orders of n .

follow the modulation signal and as a consequence higher peaks in the distribution occur. For frequencies below the optimum synchronization, the noisy background with purely statistical transitions between L and H state mainly determines the system.

In Fig. 3 the resulting time trace signals of the output voltage V_r are shown for $f = 0.1$ Hz (upper panel), $f = 1.0$ Hz (middle panel) and $f = 1.8$ Hz (lower panel). For $f = 0.1$ Hz one can see that during one single modulation cycle a lot of noise-activated transitions occur. For $f = 1.0$ Hz, a synchronization between $V_r(t)$ and $V_g(t)$ is evident. For modulations of the input with higher frequencies a loss of synchronization occurs. For $f = 1.8$ Hz, the system cannot always follow the modulation signal and remains in the state often longer than one signal period.

Another indication for SR is shown in Fig. 4, where the area P_1 under the first peak for the first residence time as a function of the frequency of the periodic forcing is plotted. P_1 is defined by

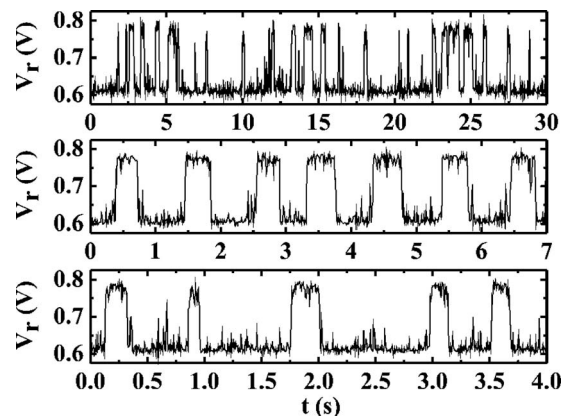


FIG. 3. Time trace signals of the output voltage V_r for different external signal frequencies: $f = 0.1$ Hz (upper graph), $f = 1.0$ Hz (middle graph), $f = 1.8$ Hz (lower graph). At $f = 1$ Hz the noise dynamics follow directly the frequency of the external input forcing with a maximum synchronization. For this frequency the time matching condition of SR is fulfilled.

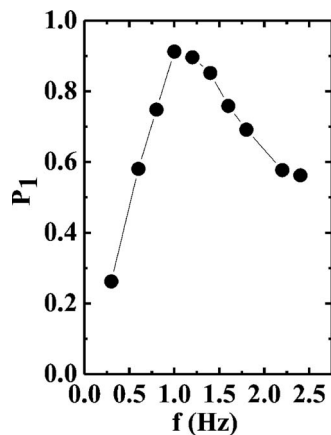


FIG. 4. Distribution of the area P_1 (first peak area) after Eq. (2) as a function of the frequency of the periodic forcing. A maximum P_1 is achieved at the SR frequency of $f=1$ Hz.

$$P_1 = \int_{T_1 - \alpha T_\omega}^{T_1 + \alpha T_\omega} N_L(T) dT, \quad (2)$$

with $n=1, 2, \dots$ and $0 < \alpha = 0.2 \leq 0.25$. The pronounced maximum at $f \approx 1.0$ Hz verifies that background floor of the three-terminal nanojunction can be fully synchronized with an external added periodic forcing.

In summary, synchronization between the internal noise floors of a bistable Y-branch switch with a weak external periodic forcing was demonstrated. This modulation frequency fulfils the time matching condition of SR. We stress the fact that such a synchronization has been obtained without acting on the intrinsic noise floor, as it was customary in earlier demonstration of nanoscale SR [see e.g., in Ref. 16] but by acting solely on the external periodic signal accessible

parameters (dc component and frequency). This operating condition opens-up interesting opportunities for designing nanoscale devices in the presence of noise floor intensities that have been considered prohibitive to date.

This work is supported by the European Commission (IST-034236 SUBTLE) and the state of Bavaria. Expert technical assistance by M. Emmerling and S. Kuhn is gratefully acknowledged.

¹L. Gammaitoni, P. Hänggi, P. Jung, and F. Marchesoni, *Rev. Mod. Phys.* **70**, 223 (1998).

²R. Benzi, A. Sutera, and A. Vulpiani, *J. Phys. A* **14**, L453 (1981).

³R. Benzi, G. Parisi, A. Sutera, and A. Vulpiani, *Tellus* **34**, 10 (1982).

⁴B. McNamara, K. Wiesenfeld, and R. Roy, *Phys. Rev. Lett.* **60**, 2626 (1988).

⁵J. F. Lindner, M. Bennet, and K. Wiesenfeld, *Phys. Rev. E* **72**, 051911 (2005).

⁶J. E. Levin and J. P. Miller, *Nature (London)* **380**, 165 (1996).

⁷J. K. Douglass, L. Wilkens, E. Pantazelou, and F. Moss, *Nature (London)* **365**, 337 (1993).

⁸L. Gammaitoni, P. Hänggi, P. Jung, and F. Marchesoni, *Eur. Phys. J. B* **69**, 1 (2009).

⁹S. Reitzenstein, L. Worschech, P. Hartmann, M. Kamp, and A. Forchel, *Phys. Rev. Lett.* **89**, 226804 (2002).

¹⁰D. Hartmann, L. Worschech, and A. Forchel, *Phys. Rev. B* **78**, 113306 (2008).

¹¹J.-O. J. Wesström, *Phys. Rev. Lett.* **82**, 2564 (1999).

¹²D. Hartmann, L. Worschech, S. Lang, and A. Forchel, *Electron. Lett.* **41**, 1083 (2005).

¹³F. Hartmann, D. Hartmann, P. Kowalzik, L. Gammaitoni, A. Forchel, and L. Worschech, *Appl. Phys. Lett.* **96**, 082108 (2010).

¹⁴L. Gammaitoni, F. Marchesoni, E. Menichella-Saetta, and S. Santucci, *Phys. Rev. Lett.* **62**, 349 (1989).

¹⁵A. Papoulis, *Probability, Random Variables and Stochastic Processes* (McGraw-Hill, New York, 2002).

¹⁶R. L. Badzey and P. Mohanty, *Nature (London)* **437**, 995 (2005).